# Viral Blips of HIV

s161463 Benjamin Jüttner
s160412 Arturo Arranz
s151499 Stanislav Valentinov Karadatchki

December 28, 2017

## 1 Introduction

This project analyses the work of [ZWY14] which presents several ODE models for *viral blips* in HIV(Human Immunodeficiency Virus)-infections. After providing a biological overview in section 2.1 we focus on one of the models especially. We clarify how a *homoclinic bifurcation* could explain the blips in section 2.3. The authors say that the viral blips are not due to a homoclinic bifurcation because no homoclinic orbit can exist. We explain in section 2.5 how the authors prove this nonexistence for the model. In section 4 we explain how we prove the nonexistence for certain choices of the parameters and in section 3 we show where we - in contrast to the authors - *do* find a homoclinic orbit numerically.

## 2 Modelling

### 2.1 The underlying biology

*Viral blips* are sudden peaks in the viral load while the load is a measure for the quantity of the virus per unit of volume[1]. The HI-virus befalls the $CD4^+$-T cells in particular, and their infection can be *productive* or *latent*. In the productive state, the $CD4^+$-T cells produce new viral particles, thus increasing the viral load. In the latent state, the infected cells don't produce new viral particles [2].

The 3-D-model in 3.1 and 3.2.1 of [ZWY14] is given by

$$\frac{dX}{d\tau} = 1 - D_x X - (B + \tfrac{AR}{R+C})XY \quad C = 3.94 \cdot 10^{-4} \tag{1}$$

$$\frac{dY}{d\tau} = (B + \tfrac{AR}{R+C})XY - Y \tag{2}$$

$$\frac{dR}{d\tau} = Y - D_r R \qquad D_r = 1000 \tag{3}$$

where $X$ and $Y$ are the populations of uninfected and infected $CD4^+$-T cells and $R$ is an amount of general "damage caused by the infection". The model uses the concept of a so-called infectivity function $B + \frac{AR}{R+C}$, which contributes positively to the growth rate of the infected cells and negatively to the growth rate of the uninfected cells. Moreover, the model has the uninfected cells produced regardless of other influences, at a constant production rate (the 1 in eqn. 1) Then they let the uninfected cells die "naturally" (independent of infection) as a percentage of the uninfected population

[1] [ZWY14], [WVL17]
[2] [WVL16]

(the term $-D_x X$ in eqn. 1). In eqn. 4.2 of [ZWY14] a 2-D-model is presented[3] as well:

$$\frac{dX}{dt} \equiv \dot{X} = 1 - DX - (B + \frac{AY}{Y+C})XY \tag{4}$$

$$\frac{dY}{dt} \equiv \dot{Y} = (B + \frac{AY}{Y+C})XY - Y \tag{5}$$

$$A = 0.364 \;\; C = 0.823 \;\; D = 0.057,$$

The variables and coefficients have exactly the same biological meanings as in the 3-D-model but lacks the "general damage". Here the infectivity function depends on $Y$ instead. It is always multiplied by both the number of infected and the uninfected cells, since the infected cells can spawn no more if there are no healthy cells left, whereas without *infected* cells the healthy cells are unharmed by the infectivity. Last but not least, the infected cells do not arise out of nowhere (i.e. the model does not account for the initialization of the infection), so their growth rate is zero if their population is zero. In section 2.2 we present a way of reducing the 3-D-model to the system (4,5).

## 2.2 Model reduction: 3D to 2D

We introduce the scaling $R = \epsilon\tilde{R}$, $C = \epsilon\tilde{C}$, $\tau = \epsilon t$, $\epsilon = D_r^{-1}$, where $\epsilon << 1$. The scaling is coherent because $C$ is small in eqns. 1 to 3 and $D_r$ is big. Moreover, in eqn. 3, $R$ reduces fast due to the high $D_r$, so we interpret $R$ as the fast variable and $X$ and $Y$ as the slow variables. Since $\frac{AR}{R+\epsilon\tilde{C}} = \frac{A\epsilon\tilde{R}}{\epsilon\tilde{R}+\epsilon\tilde{C}} = \frac{A\tilde{R}}{\tilde{R}+\tilde{C}}$, eqns. 1 to 3 can be rewritten as

$$\frac{dX}{d\tau} = 1 - D_x X - (B + \frac{A\tilde{R}}{\tilde{R}+\tilde{C}})XY \tag{6}$$

$$\frac{dY}{d\tau} = (B + \frac{A\tilde{R}}{\tilde{R}+\tilde{C}})XY - Y \tag{7}$$

$$\epsilon\frac{d\tilde{R}}{d\tau} = Y - D_r\epsilon\tilde{R} = Y - \tilde{R} \tag{8}$$

Since $t = \tau/\epsilon$, we know that $\frac{d()}{d\tau} = \dot{()}/\epsilon$ , so we can write

$$\dot{X} = \epsilon(1 - D_x X - (B + \frac{A\tilde{R}}{\tilde{R}+\tilde{C}})XY) \tag{9}$$

$$\dot{Y} = \epsilon((B + \frac{A\tilde{R}}{\tilde{R}+\tilde{C}})XY - Y) \tag{10}$$

$$\dot{\tilde{R}} = Y - \tilde{R} \tag{11}$$

Now we are able to apply the Slow-Fast theory from [VP16], dividing our system in *Layer and Reduced problems*. The *layer problem* is now obtained by setting $\epsilon = 0$ in eqns 9 to 11:

$$\dot{X} = 0 \quad \dot{Y} = 0 \quad \dot{\tilde{R}} = Y - \tilde{R}, \tag{12}$$

The Jacobian of the fast subsystem with respect to the fast variables, i.e. the Jacobian of $Y - \tilde{R}$ with respect to $\tilde{R}$, is easily seen to be -1, so the normal hyperbolicity condition is fulfilled. The critical manifold $C_0$ is the set of all fixed points of 12, i.e. the points for which $\tilde{R} = Y$ holds:

$$C_0 : \tilde{R} = Y \equiv h_0(Y) \tag{13}$$

[3]The authors denoted the temporal variable with $\tau$ in eqns. (4,5), however we renamed it to $t$, as $\tau$ is reserved for the slow-fast analysis in section 4.

If we consider eqns 6 to 8 for $\epsilon = 0$, we obtain the *reduced problem* with eqns 6 and 7 unchanged and

$$0 = Y - \tilde{R} \tag{14}$$

Now by Theorem 1 of [VP16], the fast variables can be expressed in terms of the slow variables :

$$\tilde{R} = h_0 + \mathcal{O}(\epsilon) \tag{15}$$

In general, $h_0$ depends on all the slow variables, while we can see from eqn. 13 that here it only depends on $Y$. So we arrive at

$$\tilde{R} = Y + \mathcal{O}(\epsilon), \tag{16}$$

where the $\mathcal{O}(\epsilon)$-terms can be neglected. Then plugging $\tilde{R} = Y$ into eqns. 6 and 7, and renaming $\tau$ to $t$ and $\tilde{C}$ to $C$, we arrive at eqns. (4,5).

## 2.3 How a Homoclinic Orbit can explain viral blips

The viral blips separated by long periods of quiescence in viral reproduction correspond to a periodic signal and thus a closed orbit in the phase portrait. The length of the quiescent sections is explained by a relatively small distance of the phase point from a saddle equilibrium: The dynamics slow down close to the saddle since an equilibrium is never reached before infinite time. The limit cycle is close to (far from) the saddle in a region of the phase plane that corresponds to a low (high) viral load. In the limit where the periodic orbit intersects with the saddle, it becomes a homoclinic orbit.

## 2.4 Classification of equilibria and bifurcation diagram

In system (4,5) we treat $B$ as a bifurcation parameter. The first equilibrium (denoted $E_0$) is found by considering that $Y = 0$ implies $\dot{Y} = 0$. Then for $\dot{X}$ to be 0, $X = D^{-1}$ has to be fulfilled. Thus

$$E_0 = (D^{-1}, 0) \tag{17}$$

Similarly, by setting $\dot{X} = \dot{Y} = 0$ and $Y \neq 0$, we get the two other equilibria[4]

$$E_1 = \begin{bmatrix} \frac{\sqrt{-2D(2AC+A+BC+B)+(A+BC+B)^2+D^2}+A+BC+B+D}{2D(A+B)} \\ -\frac{\sqrt{-2D(2AC+A+BC+B)+(A+BC+B)^2+D^2}-A+B(C-1)+D}{2(A+B)} \end{bmatrix} \tag{18}$$

$$E_2 = \begin{bmatrix} \frac{-\sqrt{-2D(2AC+A+BC+B)+(A+BC+B)^2+D^2}+A+BC+B+D}{2D(A+B)} \\ \frac{\sqrt{-2D(2AC+A+BC+B)+(A+BC+B)^2+D^2}+A-B(C-1)-D}{2(A+B)} \end{bmatrix} \tag{19}$$

The Jacobian of system (4,5) is easily calculated to be

$$J = \begin{bmatrix} -Y\left(\frac{AY}{C+Y}+B\right) - D & \frac{AC^2X}{(C+Y)^2} - X(A+B) \\ Y\left(\frac{AY}{C+Y}+B\right) & \frac{AXY(2C+Y)}{(C+Y)^2} + BX - 1 \end{bmatrix} \tag{20}$$

For $E_0$, the matrix $J$ becomes simple and the eigenvalues are $\{-D, \frac{B}{D} - 1\}$. This means that $E_0$ is a stable node for $B < D$ and a saddle for $B > D$. The eigenvector that corresponds to the always stable eigenvalue $-D$ is $(1, 0)$. This means that whenever $E_0$ is a saddle, its stable subspace is tangential to the $X$-axis. In fact it is even identical to the $X$-axis, as $Y = 0$ is a solution trajectory of system (4,5).

[4]The authors do not make a distinction between these two equilibria but denote the entirety of them by $E_1$. In our opinion, this is not precise enough, since $E_1$ is affected by the transcritical, while $E_2$ is affected by the Andronov-Hopf-bifurcation.

For $E_1$ and $E_2$ we calculated the Jacobian in these points and the respective eigenvalues with Mathematica. However we found out that a closed-form expression of these eigenvalues is very lengthy, so we did the analysis using plots of the eigenvalues in the complex plane. We also created scripts in MATLAB and Mathematica that show the location and the stability of the equilibria as $B$ changes. There are two bifurcations mentioned by the authors and on e bifurcation found by us:

Firstly, in [ZWY14] a transcritical bifurcation is presented. By plugging $B = D$ into eqn. 18, it can easily be verified that in this case $E_1$ coincides with $E_0$. With the scripts we found that $E_1$ is a saddle for $B < D$ and a stable node for $B > D$ Moreover, $E_1$ lies above (below) the $X$-axis for $B < D$ ($B > D$).

Secondly, the authors mentioned an Andronov-Hopf-bifurcation that happens at $B \approx 0.121$. With the scripts we found that $E_2$ is an unstable (stable) focus for $B < 0.121$ ($B > 0.121$).

Lastly, it can be seen from eqns. 18 and 19 that the locations of $E_1$ and $E_2$ coincide when the term under the square root becomes 0. Solving for $B$ reveals that this is the case when $B = -0.311765$ and $B = -0.0250426$. Thus a *saddle-node-bifurcation* happens at these values. For $B$ between these two values, the locations of $E_1$ and $E_2$ are not purely real-valued, so the two equilibria do not exist there. However we did not consider $B < 0$ biologically relevant.

### 2.5 How the authors disprove a homoclinic orbit

The authors make their point based on $E_0$. Their argumentation[5]:

[i ] $E_0$ is a saddle with the vector $(1, 0)$ spanning the stable subspace.

[ii ]The $X$-axis is not only tangential to the stable subspace but it actually is a solution curve of the system (4,5).

[iii ] In a homoclinic orbit, the flow has to start on the *unstable* manifold of the saddle and come back via its *stable* manifold (in forward time).

[iv ] because of argument [ii] the flow cannot join the $X$-axis if it started outside the $X$-axis (uniqueness of solutions). $\Rightarrow$ No homoclinic orbit.

We agree with this argumentation because a homoclinic orbit requires a saddle, and we have explained in 2.4 that there is exactly one saddle in the system for each $B < D$ and for each $B > D$. However, for $B < D$ the saddle is *not* in the point $E_0$, so argument [i] breaks down here. Because of this, we devote section 4 to proving that there can be no homoclinic orbit for $B < D$ either.

## 3 Numerical Analysis

### 3.1 Bifurcation and periodic orbits analysis

The aforementioned bifurcations in section 2.4 are confirmed with the numerical simulations of the 2D model. In figures 1a and 1b are compared the bifurcation diagrams of the authors and the diagram generated with the software AUTO.

In fig. 1b the points 4,3 and 2 correspond to a *Transcritical, Saddle-Node-* and *Andronov-Hopf-bifurcation* respectively. Both graphs have the same values, hence we were able to successfully reproduce their results.

The *saddle-node bifurcation* has a value of $B = -0.0025$, which is not biologically possible, since $B$ represents a population. Therefore this bifurcation is not longer analysed.

However, the Transcritical and Andronov-Hopf-bifurcations will play an important role in the dynamics of the system and in our aim to find a Homoclinic orbit. The transcritical bifurcation is responsible for changing the stability and location of the Saddle equilibrium needed to form the Homoclinic orbit.

[5] section 4.2.3 in [ZWY14]

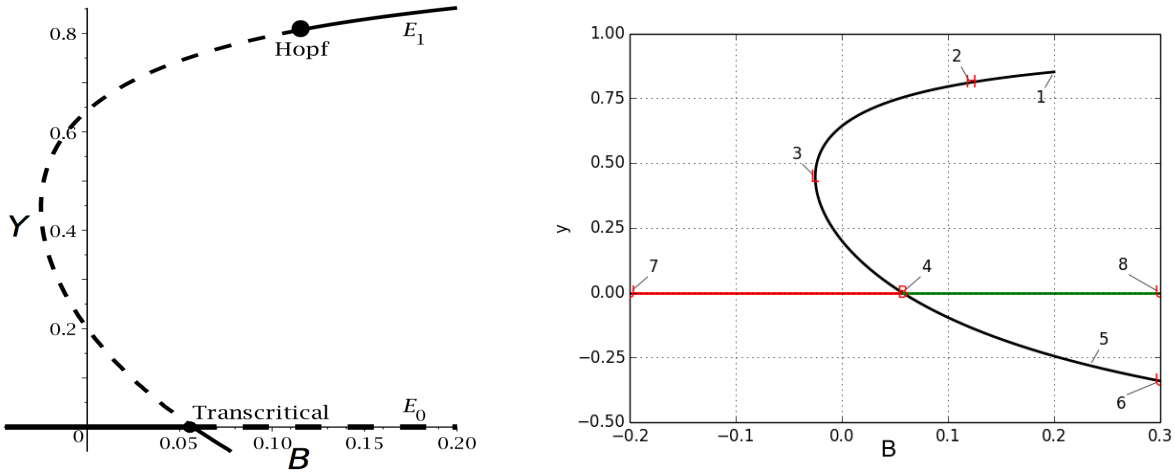


(a) From [ZWY14]

(b) AUTO generated

Figure 1: Bifurcation diagrams

On the other hand the Andronov-Hopf-bifurcationis responsible for the limit cycles which also are needed for a potential Homoclinic bifurcation. In order to categorize the Andronov-Hopf-bifurcation,

| **Bif. Type** | **B** | **X** | **Y** |
|---|---|---|---|
| Saddle-Node | -2.50426E-02 | 9.71367E+00 | 4.46321E-01 |
| Transcritical | 5.70000E-02 | 1.75439E+01 | 7.34166E-08 |
| Andronov-Hopf | 1.20986E-01 | 3.31506E+00 | 8.11042E-01 |

Table 1: Bifurcation values

the limit cycles were calculated for different values of $B$. In figure 2a the maximum $Y$ with respect the bifurcation parameter is represented. Of course, for the equilibrium points represented by the red-and-green line ($E_0$) and the black line ($E_1$ and $E_2$), the maximum $Y$ is $Y$ itself. However, the blue line represents the maximum $Y$ that each of the found periodic orbits reaches. The labels 9 to 19 correspond to such periodic orbits.
Now the type of Hopf-bifurcation is clear. To the left of the of the bifurcation we have a unstable focus and limit cycles. To the right of the bifurcation we have a stable focus and no limit cycles. This is a *Supercritical Andronov-Hopf-bifurcation.*

In fig. 2b, the periodic orbits are represented in the phase portrait. For small values of $B$ we have big orbits, which approach the shape of a Homoclinic orbit. As we increase $B$ we get smaller orbits, which finally disappear.

An important observation in the simulations is the following: the periodic orbits only appear between a bit before the transcritical and the Hopf, i.e. from $B \approx 0.057$ to $B \approx 0.12$. We know what makes them disappear, but what makes them appear in the first place? For answering this question it is necessary to take a look closer at the Transcritical bifurcation.

## 3.2 Numerical evidence of Homoclinic orbit

The information relative to the periodic orbits can be seen in table 2. For small values of $B$ and very close to the left side of the Transcritical bifurcation there are big orbits with big periods. For bigger values of $B$ we have smaller orbits and smaller periods. However, the relation between the size and the period is not linear, but rather exponential.

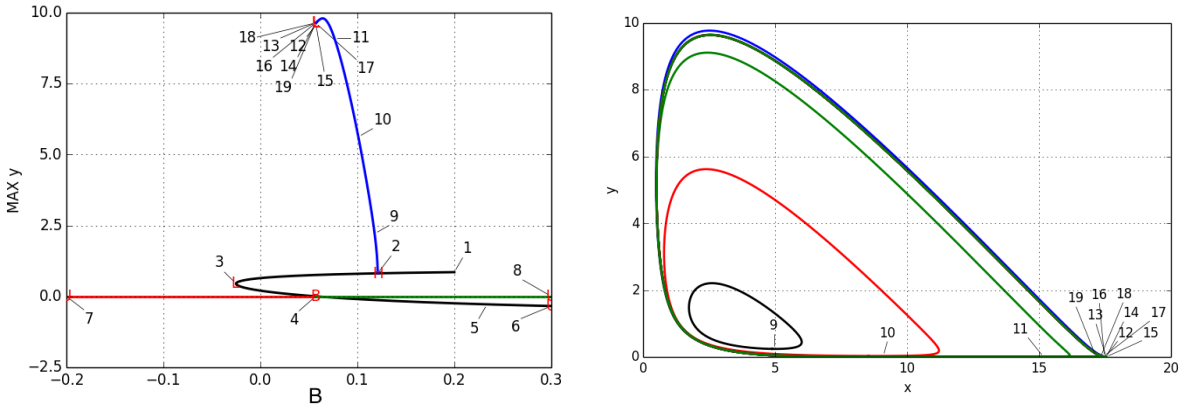


(a) Periodic orbits in the bifurcation diagram

(b) Periodic orbits in the phase portrait

Figure 2: Periodic orbits for different values of B

| Label | B | max X | max Y | Period |
|---|---|---|---|---|
| 9 | 1.17837E-01 | 6.00893E+00 | 2.20656E+00 | 1.50378E+01 |
| 10 | 1.01042E-01 | 1.12065E+01 | 5.61789E+00 | 2.46433E+01 |
| 11 | 7.62963E-02 | 1.61601E+01 | 9.10364E+00 | 5.28157E+01 |
| 12 | 6.16998E-02 | 1.75190E+01 | 9.76291E+00 | 1.55451E+02 |
| 13 | 5.72371E-02 | 1.75438E+01 | 9.63886E+00 | 1.97765E+03 |
| 14 | 5.69999E-02 | 1.75439E+01 | 9.63113E+00 | 1.60562E+06 |
| 15 | 5.69999E-02 | 1.75439E+01 | 9.63111E+00 | 1.49245E+09 |
| 16 | 5.69999E-02 | 1.75439E+01 | 9.63112E+00 | 1.98269E+09 |

Table 2: Periodic orbits

The interesting orbits, as we said, are the ones close to $B \approx 0.057$. In figures 3a and 3b we show the dynamics of the orbit 16 and 12 very close to the region where the Transcritical bifurcation happens. The green dot represents $E_1$ while the blue is $E_0$. In figure 3a, $E_1$ is still a saddle and the periodic orbit crosses through it. This is apparently a contradiction of uniqueness. However, the period, with value t=1.98269E+09, is very big which implies that the orbit is actually infinitesimally close to the equilibrium and we lack precision in our plots to show such distance.
In figure 3b the Transcritical has already happened ($B > D$). The periodic orbit in this case approaches $E_0$ (blue dot), but does not touch it. This agrees with the fact that the periodic orbit does not touch the x axis, but rather exponentially close to it, hence the orbit is not in the stable manifold of $E_0$. Once that it gets close enough to the point it is repelled, since now $E_0$ is a saddle.

As aforementioned, the period increases exponentially with decreasing $B$. This is represented in figure 4 where the period is plotted with respect to the bifurcation parameter. The plot suggests that periodic cycles are 'born' from infinite period orbits. The exponentially close distance between some periodic orbits and $E_1$ **strongly suggests a Homoclinic Bifurcation very close to the left side of** $B = 0.057$.

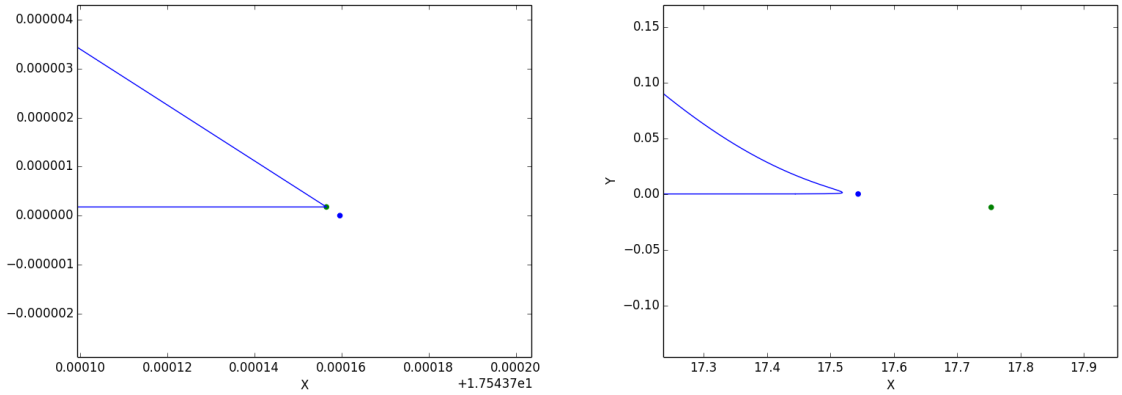


(a) Orbit 16, occurs before the Transcritical bifurcation (b) Orbit 12, occurs after the Transcritical bifurcation

Figure 3: Zoomed periodic orbits

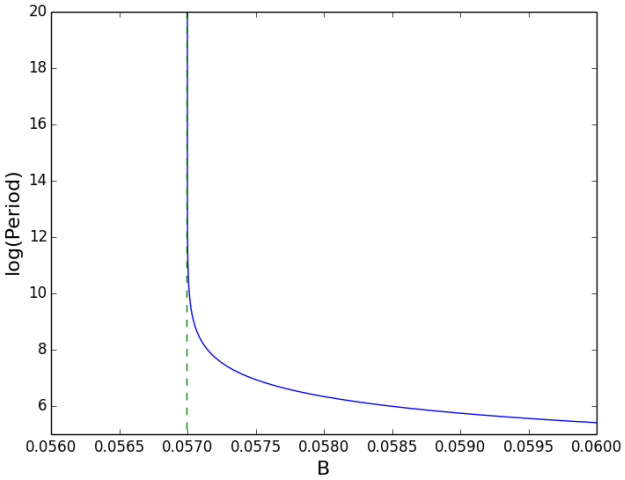


Figure 4: Period of orbits with respect to B

# 4 Analysis

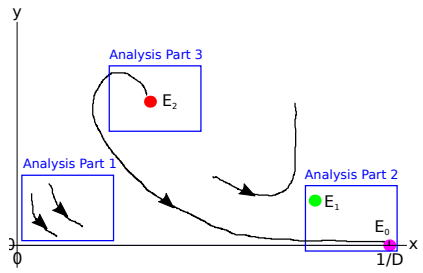


Figure 5: Regions of the phase space that the rescaled systems in this section 'zoom into'

This analysis is divided into three parts. Each part focuses on a different region of the phase portrait as indicated by figure 5. The second and third parts involve slow-fast analysis. The final goal is to prove whether or not a homoclinic orbit exists. For convenience, $X$ and $Y$ from eqns. (4,5) are renamed into $x$ and $y$ in this section.

In order to perform slow-fast analysis on the system of equations

$$\dot{x} = g(x, y)$$
$$\dot{y} = f(x, y)$$

the system is first scaled using $0 < \epsilon << 1$

$$\dot{x} = g(x, y)\epsilon \qquad \dot{x} = g(x, y)$$
$$\dot{y} = f(x, y), \qquad \epsilon\dot{y} = f(x, y)$$

The system is then analyzed in two singular limits known as the layer problem

$$\dot{x} = 0$$
$$\dot{y} = f(x, y)$$

and the reduced problem

$$\dot{x} = g(x, y)$$
$$0 = f(x, y)$$

with $\epsilon = 0$.
In both cases the variables x and y must be scaled by $\epsilon$. In the reduced problem the time t is scaled by $\epsilon$ as well. Coefficients inside $g$ and $f$ may be scaled as well. It is important to ensure that the system has normal hyperbolicity. This is equivalent to $D_y f(x, y) \neq 0$. After the analysis for $\epsilon = 0$ is done, the results are put together into one combined phase portrait where $\epsilon > 0$ again. This analysis gives a very accurate approximation to the original system.

## 4.1 Analysis Part 1

Rescale the B, D, and A coefficients:

$$B = b\epsilon^2 \quad D = \epsilon^2 \quad A = a\epsilon$$

System of equations with rescaled coefficients:

$$\dot{x} = 1 - \epsilon^2 x - (b\epsilon^2 + \frac{a\epsilon y}{y+c})xy \tag{21}$$

$$\dot{y} = (b\epsilon^2 + \frac{a\epsilon y}{y+c})xy - y \tag{22}$$

$$\epsilon = 0$$

$$\dot{x} = 1 \tag{23}$$

$$\dot{y} = -y \tag{24}$$

$$x = t + x_0$$

$$y = e^{-t} y_0 \tag{25}$$

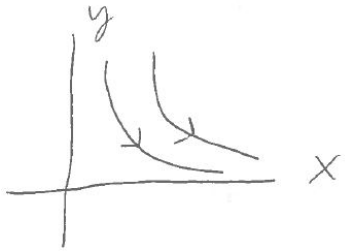


Figure 6

The infected cell population density goes to zero; and the uninfected cell population density goes to infinity. In order to obtain a more accurate system approximation slow-fast analysis is needed.

## 4.2 Analysis Part 2

Rescale x and y:

$$\hat{x} = \epsilon\tilde{x}$$

$$\epsilon\hat{y} = \tilde{y}$$

System of equations with rescaled variables:

$$\dot{\hat{x}} = \epsilon^2 - \epsilon^2\hat{x} - (b\epsilon^3 + \frac{a\epsilon^3\hat{y}}{\epsilon\hat{y}+c})\hat{x}\hat{y} \tag{26}$$

$$\dot{\hat{y}} = (b + \frac{a\hat{y}}{\epsilon\hat{y}+c})\hat{x}\hat{y} - \hat{y} \tag{27}$$

Layer Problem

$$\epsilon = 0$$

$$\dot{\hat{x}} = 0 \tag{28}$$

$$\dot{\hat{y}} = (b + \frac{a\hat{y}}{c})\hat{x}\hat{y} - \hat{y} \tag{29}$$

The set of equilibria for this system corresponds to the critical manifold

$$\hat{x} = \hat{x}_0 \tag{30}$$

$$0 = (b + \frac{a\hat{y}}{c})\hat{x}\hat{y} - \hat{y} \tag{31}$$

$$\hat{y} = \frac{c}{\hat{x}a} - \frac{bc}{a}, \hat{y} = 0 \tag{32}$$

These two lines intersect at $\frac{1}{b}$

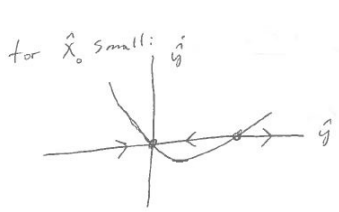


Figure 7

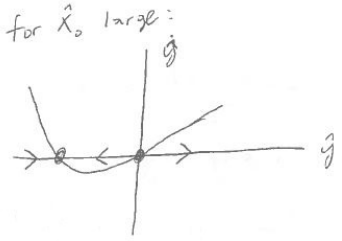


Figure 8

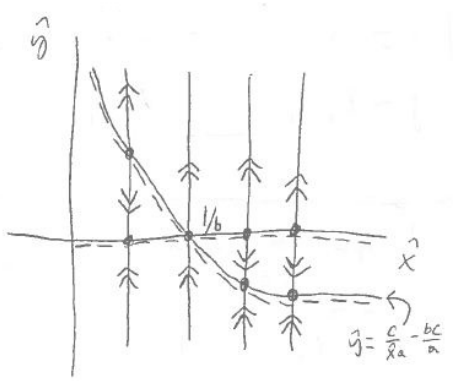


Figure 9: Layer Problem Phase Portrait

The system has normal hyperbolicity along the critical manifold except at $\hat{x} = \frac{1}{b}$.

Reduced Problem

$\tau = t\epsilon^2$, $t = \tau\epsilon^{-2}$
The new system of equations is

$$\dot{\hat{x}} = 1 - \hat{x} - (b\epsilon + \frac{a\epsilon\hat{y}}{\epsilon\hat{y} + c})\hat{x}\hat{y} \tag{33}$$

$$0 = (b + \frac{a\hat{y}}{\epsilon\hat{y} + c})\hat{x}\hat{y} - \hat{y} \tag{34}$$

$$\epsilon = 0$$

$$\dot{\hat{x}} = 1 - \hat{x} \tag{35}$$

$$0 = (b + \frac{a\hat{y}}{c})\hat{x}\hat{y} - \hat{y} \tag{36}$$

Equilibria

Critical manifold

$$\hat{y} = \frac{c}{\hat{x}a} - \frac{bc}{a}, \hat{y} = 0 \tag{37}$$

$$\hat{x} = 1 \tag{38}$$

$$\hat{y} = 0, \hat{y} = \frac{c - bc}{a} \tag{39}$$

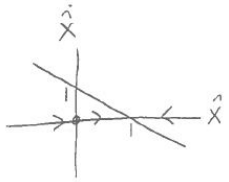


Figure 10

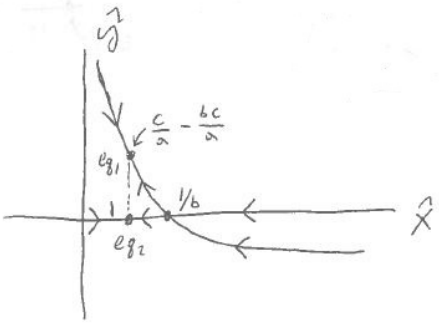


Figure 11: b<1

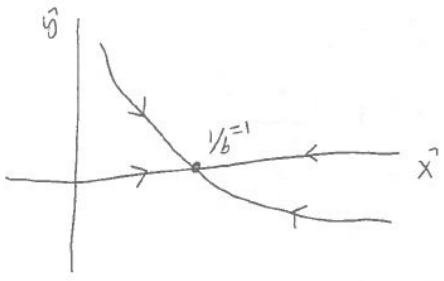


Figure 12: b=1

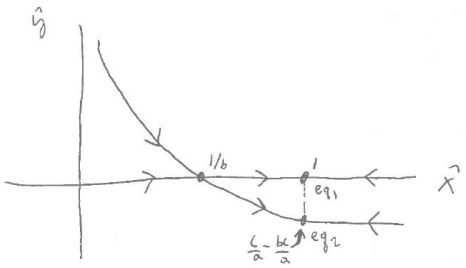


Figure 13: b>1

Combined System

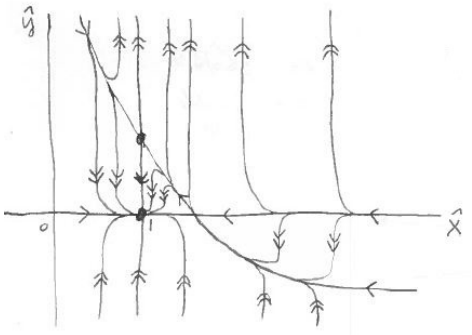


Figure 14: b<1 equilibrium 1 saddle, equilibrium 2 stable node

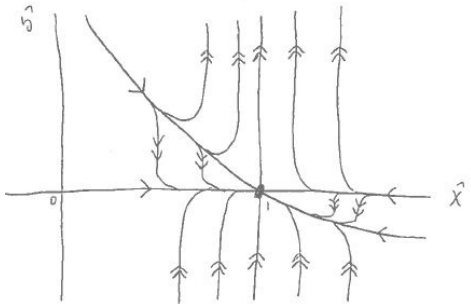


Figure 15: b=1 one equilibrium

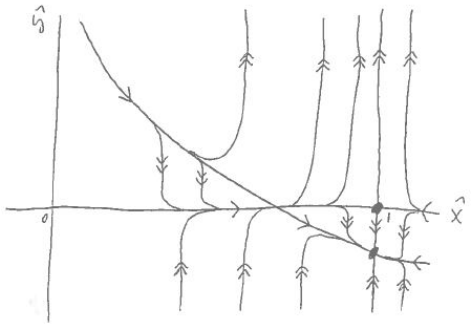

Figure 16: b>1 equilibrium 1 stable node, equilibrium 2 saddle

### 4.3 Analysis Part 3

$$\hat{x} = \epsilon\tilde{x}$$
$$\epsilon\hat{y} = \tilde{y}$$
$$\dot{\tilde{x}} = \epsilon - \epsilon^2\tilde{x} - (b\epsilon^2 + \frac{a\epsilon\tilde{y}}{\tilde{y}+c})\tilde{x}\tilde{y} \tag{40}$$
$$\dot{\tilde{y}} = (b\epsilon + \frac{a\tilde{y}}{\tilde{y}+c})\tilde{x}\tilde{y} - \tilde{y} \tag{41}$$

Layer Problem

$$\epsilon = 0$$
$$\dot{\tilde{x}} = 0 \tag{42}$$
$$\dot{\tilde{y}} = \frac{\tilde{y}a}{\tilde{y}+c}\tilde{x}\tilde{y} - \tilde{y} \tag{43}$$

The set of equilibria for this system corresponds to the critical manifold

$$\dot{\tilde{x}} = \tilde{x}_0 \tag{44}$$
$$0 = \frac{\tilde{y}a}{\tilde{y}+c}\tilde{x}\tilde{y} - \tilde{y} \tag{45}$$
$$\tilde{y} = \frac{c}{\tilde{x}a - 1}, \tilde{y} = 0 \tag{46}$$

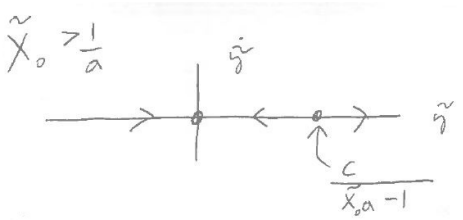

Figure 17

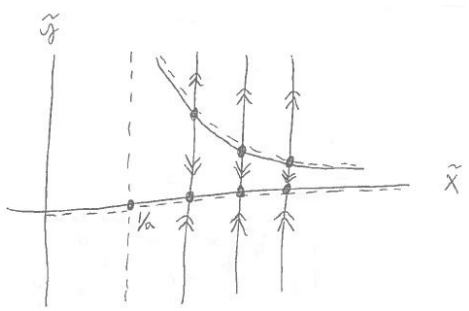

Figure 18: Layer Problem Phase Portrait

The system has normal hyperbolicity along the critical manifold except at $\tilde{x} = \frac{1}{a}$.

Reduced Problem

$\tau = t\epsilon$, $t = \tau\epsilon^{-1}$
The new system of equations is

$$\dot{\tilde{x}} = 1 - \epsilon\tilde{x} - (b\epsilon + \frac{a\tilde{y}}{\tilde{y}+c})\tilde{x}\tilde{y} \tag{47}$$

$$0 = (b\epsilon + \frac{a\tilde{y}}{\tilde{y}+c})\tilde{x}\tilde{y} - \tilde{y} \tag{48}$$

$$\epsilon = 0$$

$$\dot{\tilde{x}} = 1 - \frac{a\tilde{x}\tilde{y}^2}{\tilde{y}+c} \tag{49}$$

$$0 = \frac{\tilde{x}\tilde{y}^2 a}{\tilde{y}+c} - \tilde{y} \tag{50}$$

Critical Manifold

$$\tilde{y} = \frac{c}{\tilde{x}a - 1}, \tilde{y} = 0 \tag{51}$$

Equilibrium

$$\tilde{x} = \frac{1+c}{a}, \tilde{y} = 1 \tag{52}$$

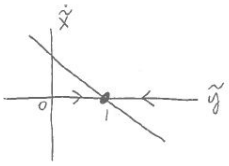

Figure 19

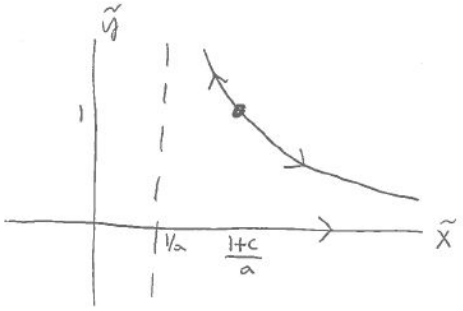


Figure 20: Reduced Problem Phase Portrait

Combined System

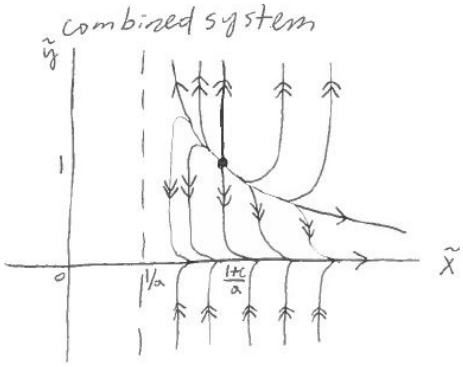


Figure 21: unstable node equilibrium

Final Result

For large x,

$$\tilde{y} = \frac{c}{a\tilde{x} - 1} \approx \frac{c}{a\tilde{x}}$$
$$\tilde{y} = \epsilon\hat{y} \approx \frac{c\epsilon}{a\hat{x}}$$
$$\hat{y} \approx \frac{c}{a\hat{x}}$$

From the $\hat{x}$ system, for small x,

$$\hat{y} = \frac{c}{a\hat{x}} - \frac{bc}{a} \approx \frac{c}{a\hat{x}}$$

Therefore for small x and b<1 the critical manifold $\hat{y} = \frac{c}{\hat{x}a} - \frac{bc}{a}$ of the $\hat{x}$ system connects to the critical manifold of the $\tilde{x}$ system.

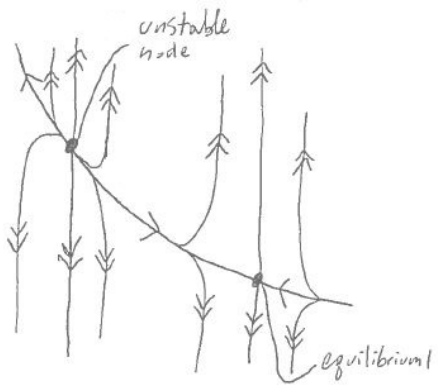


Figure 22

As we go backwards in t along the stable manifold of equilibrium 1 we reach an unstable node. Therefore there can be no homoclinic orbit for b<1.

## 4.4 Numerical confirmation of the final result

In 4.1 to 4.3 we have combined all layer and reduced problems to get an approximation to the system's flow (fig. 22) In this section we confirm numerically that the actual system (4,5) - or its rescaled counterparts - behave qualitatively the same as this combination and the flow is well approximated by the critical manifold. We do this for the scaled system (26, 27) for a non-zero (but small) $\epsilon$. We use a MATLAB ODE solver to calculate a trajectory with an initial condition (IC) $(\hat{x}_0, \hat{y}_0)$.

### 4.4.1 The heteroclinic orbit

As can be seen from the final result above a heteroclinic orbit is formed between the two equilibria for b<1. First a trajectory is selected which is close to this heteroclinic orbit. For this, we set the IC near the equivalent of $E_1$ (green point in fig. 23b) and integrate *backwards* in time. We use the values

$$b = 0.7 \quad \epsilon = 0.01 \quad \hat{x}_0 = 0.99 \;\; \hat{y}_0 = (ca^{-1} - bca^{-1}) \cdot 13$$

The result is seen in fig. 23b: the flow (black line) converges to the critical manifold (blue line) fast and remains very close to it. As time goes by in backward direction, $\hat{y}$ becomes too large to plot in this scaling, so when $\hat{y} = 10$, i.e. $\tilde{y} = 0.1$, is reached (black square), we switch to fig. 23a in order to plot the rest of the trajectory in the $\tilde{y}$-scaling.

As fig. 22 suggests for this initial condition, the flow in fig. 23 is attracted by the critical manifold in backward time and converges to the equivalent of $E_2$ (red dot).

.

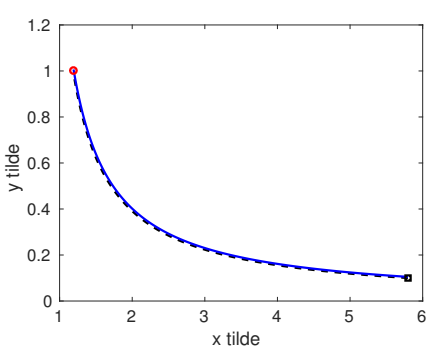


(a) $\tilde{x}, \tilde{y}$ coordinates. Red: equivalent of $E_2$

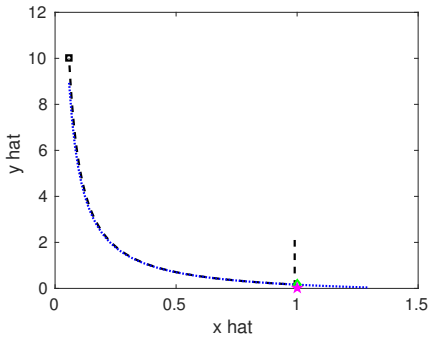


(b) $\hat{x}, \hat{y}$ coordinates. Green: equivalent of $E_1$, magenta: equivalent of $E_0$

Figure 23: Trajectory (black) of the scaled system (26, 27) near the critical manifold (blue)

### 4.4.2 The periodic orbit

Next we reproduce a periodic orbit emanating from the Andronov-Hopf-bifurcation. We choose the values

$$b = 1.1 \quad \epsilon = 0.1 \quad \hat{x}_0 = 0.8 \;\; \hat{y}_0 = 0.05$$

The result is seen in fig. 24. The IC (black square in 24a) is chosen between the hyperbola-arm of the critical manifold (blue line) and the $\hat{x}$-axis. For this IC, fig. 16 predicts an asymptotic approach to $\hat{y} = 0$ that is fast in the beginning, combined with an increase in $\hat{x}$. The trajectory (black line) in fig. 24a behaves qualitatively in this way. It is allowed to cross the slow manifold (which is close to the critical manifold and not shown in the figure) near the point $\hat{x} = 1/b$ (cyan dot), because in $1/b$ the normally hyperbolicity condition does not hold (see section 4.2) and the Slow-Fast analysis breaks down around this point. After that, $\hat{y}$ explodes, which is in accordance with fig. 16 for $x > 1/b$. The flow then converges to the periodic orbit (the "horizontal" and "vertical" black line). The orbit does not coincide with the equivalent of equilibrium $E_0$ (magenta) although it comes close to it (24b).

Apparently, the periodic orbit returns through the $\hat{x}$-axis but in reality it comes exponentially close to it. As we demonstrated it can not cross it because of invariance. For a long time this periodic orbit is contracting towards the $\hat{x}$-axis, and after the point $1/b$ when the dynamics of the layer problem is inverted, we should expect a similar period of expansion where it remains close to the axis. However, the Unstable manifold of $E_0$ must not be crossed. This explains why the orbit is repelled right before $E_0$ (and not later).

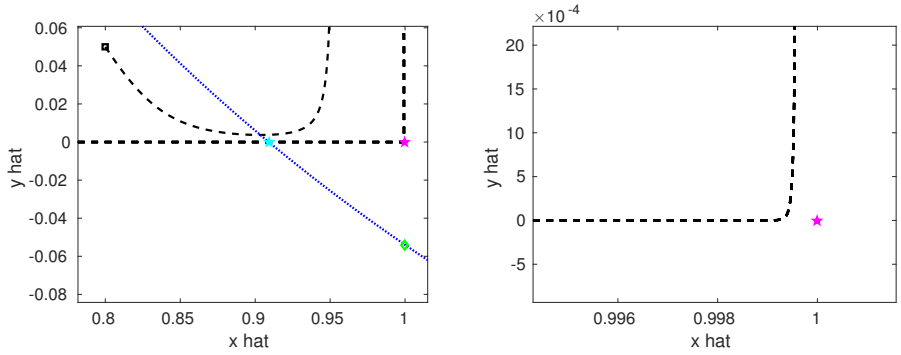


(a) cutaway showing IC and equilibria

(b) zoomed cutaway

Figure 24: Convergence to a periodic orbit in $\hat{x}, \hat{y}$ coordinates. Green: equivalent of $E_1$

# 5 Conclusion

Analytically we demonstrated the non-existence of Homoclinic orbits after the Transcritical bifurcation between $E_0$ and $E_1$. Homoclinic orbits need to departure from the unstable manifold of a saddle points and come back through the stable manifold of the same point. After the Transciritcal bifurcation $E_0$ is the saddle point. Its Stable manifold corresponds to the x axis which can never be crossed since it is an invariant set, it is a solution of the system. Hence the flow can never departure from the unstable manifold and come back through the stable manifold.

By means of Slow-Fast theory and rescaling we demonstrated in section 4 that a Heteroclinic orbit connects $E_2$ and $E_1$ for $B < D$. Hence, the analytical analysis concludes that if there is any Homoclinic orbit it has to be at the Transcritical bifurcation.

Numerically we got results which strongly suggest a Homoclinic orbit right before the Transcritical bifurcation. The main arguments for it are: the generated periodic orbits get exponentially close to the saddle $E_1$ and the birth of the periodic orbits start with infinity period.

Both analyses, numerical and analytical, complement each other because the analytical rules out the homoclinic for $B > D$ and $B < D$ while the numerical suggests it for $B \approx D$. The part of the analytical analysis that is responsible for the $B < D$ case, namely section 4, deals with the limit $\epsilon = 0$, whereas in reality or in the numerical analysis $0 < \epsilon << 1$ is the case. This explains why in the numerical analysis the homoclinic was found at a value of $B$ that is slightly smaller than (and not exactly equal to) $D$. We expect that $B_{hom}$ (the value of $B$ for which the homoclinic occurs) converges to $D$ from the left as $\epsilon \longmapsto 0$.

# References

[WVL17]

`http://www.healthline.com/health/hiv-aids/cd4-viral-count#CD4count2`

[VP16]

`Project Description of Course 01257, Kristian Uldall Kristiansen, DTU 2016`

[ZWY14] Zhang,W.,Wahl,L.M.,and Yu,P.,Viral blips may not need a trigger: How transient viremia can arise in deterministic in-host models, SIAM Review, Vol. 56, No. 1, pp. 127–155, 2014.